Analytical Methods

A Low-Interference, High-Resolution Multianalyte Electrochemical Biosensor

Journal:	*Analytical Methods*
Manuscript ID	AY-ART-03-2020-000528.R1
Article Type:	Paper
Date Submitted by the Author:	19-May-2020
Complete List of Authors:	Melow, Sara; Vanderbilt University, Chemistry; Miller, Dusty; University of California, Santa Barbara, Biomolecular Science and Engineering Program Gizzie, Evan; Vanderbilt University, Chemistry Cliffel, David; Vanderbilt University, Department of Chemistry

A Low-Interference, High-Resolution Multianalyte Electrochemical Biosensor

Sara L. Melow[1], Dusty R. Miller[1], Evan A. Gizzie[1], and David E. Cliffel[1-2*]

[1]Department of Chemistry, Vanderbilt University, Nashville, TN 37235-1822, United States
[2]Vanderbilt Institute for Integrative Biosystems Research and Education, Vanderbilt University, Nashville, TN 37235-1809, United States

*Corresponding Author:
Prof. David E. Cliffel
Department of Chemistry
Vanderbilt University
Nashville, TN 37235-1822
Tel: (615) 343-3937
Email: d.cliffel@vanderbilt.edu

Target Journal: Analyst
Reviewers: John Claussen, Janine Mauzeroll, Leslie Sombers

Abstract.

Electrochemical sensors are used by millions of patients and health care providers every year, yet these measurements are hindered by compounds that also exhibit inherent redox activity. Acetaminophen (APAP) is one such interferent that falls into this extensive class. In this work, an osmium-based redox polymer was used for electrochemical detection in a sensor that was operated at a decreased voltage, allowing for decreased interference. These sensors demonstrated better selectivity (40-fold for glucose and 200-fold for lactate) for their respective analyte over APAP, possessed higher sensitivity (0.350 ± 0.006 μA mM^{-1} for glucose and 2.00 ± 0.05 μA mM^{-1} for lactate) over a broad range of analyte concentrations (50 μM – 10 mM for glucose and 2-324 μM for lactate), and displayed similar operational stability (26% decrease for glucose and 29% decrease for lactate) over 7 days compared to first-generation sensors. To test this platform under biologically-relevant conditions, glucose metabolism was monitored in a model liver cell line, Alpha Mouse Liver 12 (AML12) after treatment with APAP and/or insulin. This work represents a high-resolution electrochemical biosensor for microphysiological monitoring of glucose and lactate in the presence of an APAP.

Introduction.

Electrochemistry is a sensitive, stable, and selective analytical tool in diagnosing and monitoring health and disease.[1–3] The most widely-used electrochemical sensors are first-generation enzymatic sensors, relying on enzymes immobilized on an electrode for analyte detection. These biosensors quantify the target analyte by means of an electroactive byproduct of the enzymatic reaction, hydrogen peroxide (H_2O_2).[4,5] For instance, glucose meters, commonly used to measure blood glucose in patients with diabetes, use first-generation sensor technology and account for the large majority of first-generation electrochemical sensors used commercially.[6] However, first-generation sensors are susceptible to electroactive interferents, compounds that lead to signal contamination and therefore inaccurate results.[7,8] In this work, a polymer was developed to act as a mediator for electron transfer, allowing for decreased interference compared to first-generation sensors. Using this polymer, we quantified glucose and lactate over a background of an inherently redox-active compound and common interferent, acetaminophen (APAP), by coupling an oxidase enzyme with this osmium redox polymer (Os-polymer) in a multianalyte sensor platform.

Although first-generation biosensors are selective for the analyte of interest against a background of electrochemically inactive species, they are still prone to interference. At the electrode surface of first-generation biosensors, H_2O_2, acting as the electron transfer mediator from the enzyme to the electrode, is oxidized with an electrode bias of 0.6 V (vs. Ag/AgCl), producing an amperometric signal.[5] However, at this potential [0.6 V (vs. Ag/AgCl)], other electroactive species such as APAP are also oxidized, causing signal interference.[7,8] Thus, biosensors that reduce or eliminate redox active interference are required for accurate analysis of the analyte of interest.

There are a number of ways to reduce or eliminate interference including screening polymers or electron transfer mediators (co-reactants).[8–10] Although screening polymers increase selectivity by preventing larger molecules from accessing the electrode surface, they still allow smaller molecules to access the electrode and contribute to signal contamination since they use a higher potential like first-

generation sensors. Furthermore, though they increase selectivity, they have decreased sensitivity due to impeded analyte diffusion.[11] However, the use of metallic co-reactants including Au, Pd, Rh, and Ru, reduce peroxide at a lower potential and therefore decrease interference.[9,12–15] Still, the instability (Rh and Pd) and expense (Au and Ru) of these materials have hamstrung their widespread implementation. Therefore, there is a need for stable and less expensive co-reactants that accurately detect analytes in all samples.

To address this need, a group of polymers that contains an osmium complex, acting as the co-reactant, were developed and incorporated into sensors. Osmium redox polymers were first developed by Heller et al. in the late 1980s to act as a mediator for electron transfer in glucose biosensors.[16] These osmium polymers are redox polymers that can be reversibly oxidized and reduced and, when they are combined with an oxidase enzyme, these polymers can stably and selectively detect their respective analyte at a lower potential, thereby decreasing interference (**Figure 1**). Previous work has shown current densities do not vary with the Os content of the polymers, so the overall redox efficiency of these sensors similarly would not change with the Os content.[17] Since their inception, their use has extended to other analytes and biological systems[18–20] such as detecting acetylcholine release from rat frontal cortex samples.[21]

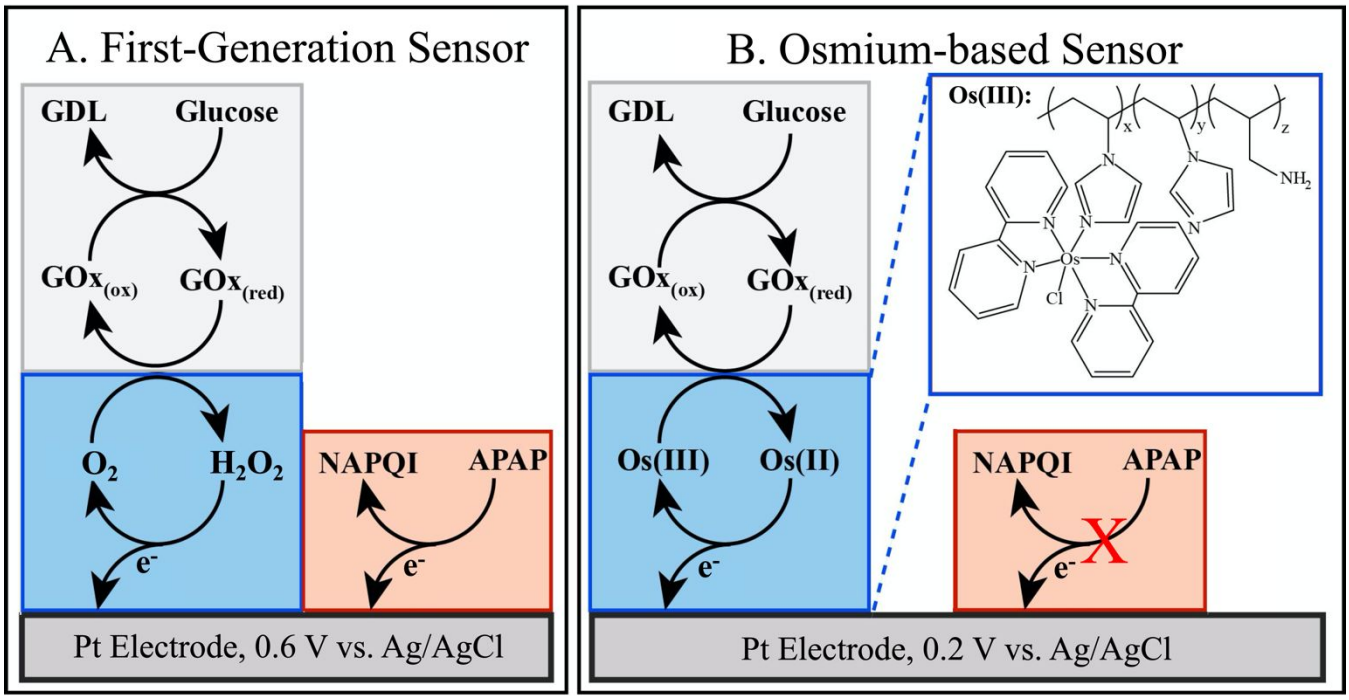

Figure 1. A) Representation of the redox process/electron flow mechanism for the first-generation GOx sensor. There is a high potential of 0.6 V (vs. Ag/AgCl) required to oxidize the H_2O_2 that also oxidizes APAP, leading to signal interference and inaccurate results. B) Representation of the redox process/electron flow mechanism for the Os-based GOx sensor. The electrode bias of 0.2 V (vs. Ag/AgCl) required for the Os-polymer and GOx system mitigates the interference from the oxidation of APAP. Inset: Representation of the Os-polymer structure.

The microclinical analyzer (μCA) provides automation, increased ease of use, real-time monitoring, and multiple analyte detection. This platform is composed of a microfluidic housing for a screen-printed electrode that is used for detection of metabolites as well as an automated pump and valve system. There is increased ease of use due to increased sample throughput and decreased user intervention from automated sensor calibration and sample input. Furthermore, the sensor and small volume-microfluidic housing allow for real-time monitoring with the ability to detect small metabolic changes.[22] Lastly, monitoring multiple analytes concurrently provides a better understanding of the cellular processes and pathways of toxicity in healthy and diseased states. This platform provides a versatile system that can be extended to many analytes and biological systems.

Because the liver has a direct role in energy and metabolism, producing, storing, and releasing glucose,[23] hepatic models are important for the comprehensive understanding of pathways and functions in the body. Alpha Mouse Liver 12 (AML12) is a cell line that models the liver and can be used to study lipid metabolism, liver injury and hepatotoxicity.[24] These cells are amply available, cost effective, and show decreased variation in quality since the cell line is both immortalized and comes from a healthy host. Furthermore, these cells most closely resemble basal and insulin-stimulated glucose metabolism in primary mouse hepatocyte cultures.[25] To answer biological questions about insulin and APAP and specifically their interactions with liver cells, glucose metabolism in a model liver system was investigated to gain insight into these relationships.

In this work, we present an Os-polymer that couples with glucose and lactate oxidases to comprise a multianalyte sensor platform for quantification that produces minimal signal interference with APAP present. Together, this system represents a new method to rapidly analyze biological systems by electrochemically monitoring cellular viability, performing toxicity screenings, and elucidating metabolic pathways. Selectivity assays demonstrated that this platform is insensitive to APAP, an electroactive interferent, and calibrations were performed in this work to cover biologically relevant linear ranges while maintaining sensitivity. Longevity studies of the sensor performance indicated that this novel platform was ideal for interfacing with continuously operational systems such as liver-on-chips. We used the AML12 cell line to study the effects of treating the cells with APAP based on its clinical relevance and hepatotoxicity, known redox activities, and insulin-dependent pathways for glucose metabolism. The platform was applied to model liver cells to detect glucose metabolism changes and monitor the effects of insulin and APAP.

Experimental

Material Procurement

N-vinylimidazole, allylamine, azobisisobutyronitrile (AIBN), 2,2'-bipyridine, ammonium hexachoroosmate (IV), poly(ethylene glycol) diglcidyl ether (PEGDGE), potassium chloride, bovine serum albumin (BSA), GOx from *Aspergillus niger* (152.54 U mg^{-1}), LOx from *Aerococcus viridians* (11.29 U mg^{-1}), and glutaraldehyde (25% by wt. aqueous solution) were purchased from Sigma Aldrich (St. Louis, MO). Sodium phosphate monobasic and sodium phosphate dibasic (buffer) were procured from Fisher Scientific (Hampton, NH). β-D-Glucose was purchased from Calbiochem (San Diego, CA), and sodium L-lactate was purchased from Alfa Aesar (Haverhill, MA) and for use in calibrations. Dulbecco's Modified Eagle Medium supplemented with F12 (DMEM/F12), glucose-free DMEM, F12, fetal bovine serum (FBS) and a primary hepatocyte maintenance supplement kit (dexamethasone, penicillin-streptomycin (p/s), insulin, transferrin, selenium complex, BSA, linoleic acid, GlutaMAX, and HEPES) were purchased from Gibco (Gaithersburg, MD). All reagents were used as received and without additional purification.

The microclinical analyzer (μCA) housing was designed by The Vanderbilt Institute for Integrative Biosystems Research and Education (VIIBRE, Nashville, TN) and made of polymethylmethacrylate by the Vanderbilt Microfabrication Core (VMFC, Nashville, TN) that is operated by VIIBRE.[26] More detailed information for the materials of this device and the screen-printed electrodes can be found elsewhere.[22] To automate the system, rotary planar peristaltic micropumps (RPPM, US patents 9,874,285 and 9,725,687 and applications claiming priority from US patent application 13/877,925), rotary planar peristaltic five-port valves (RPPV, US patent 9,618,129), microcontrollers, and computer software were implemented in the system (VIIBRE/VMFC). CHI 1440 and 1030 potentiostats were purchased from CH Instruments (Austin, TX) and used in the electrochemical measurements.

Synthesis and Characterization of the Os-based Metallopolymer

To produce the final Os-based redox polymer, $Os(bpy)_2Cl$-PVI, a polymer and an Os complex must be synthesized initially. First, the polymer backbone that connects the Os complex to the electrode, poly(N-vinylimidazole-allylamine) (PVI) was polymerized and purified. To randomly copolymerize with the N-vinylimidazole monomer and provide additional primary amine crosslinking sites, allylamine was mixed with the monomer in a 1:1 ratio (equimolar) in absolute ethanol (10-15 mL).[27] This mixture was then added to a septum-sealed round bottom flask and nitrogen purged (~15 minutes). Then, the initiator, AIBN (60:1 molar ratio of monomer to initiator), was dissolved in absolute ethanol (2-3 mL) and added through the septum to induce free radical polymerization in the reaction mixture.[28] After initiation, the reaction mixture was heated in an oil bath (85 °C, 2 hours) to complete polymerization, resulting in a solid. To remove the unwanted contaminants, ethanol (5-10 mL) was added to this solid, stirred overnight for full dissolution, and added dropwise to a beaker of rapidly stirring diethyl ether (40 mL), precipitating and purifying the PVI polymer. This purified PVI was collected on a coarse vacuum frit (Pyrex, Corning, NY), washed with cold diethyl ether (5-mL aliquots), and dried under vacuum until the solvent was fully removed (~30 minutes). The PVI was then further purified via dialysis against DI water using tubing with a 10 kDa mass limit. This PVI was used as the backbone for the Os complexes in all future experiments and was set aside until the Os complex was synthesized.

Next, the Os portion that forms the redox component of the final Os redox polymer was synthesized and purified. This synthesis was adapted from a previous method with slight changes made for this polymer.[29] Briefly, this Os redox compound, osmium[bis(2,2'-bipyridine)dichloride] ($Os(bpy)_2Cl_2$), was synthesized by refluxing (45 minutes) ammonium hexachloroosmate with two-molar equivalents of 2,2'-bipyridine in ethylene glycol (~50 mL) in a 100-mL round bottom flask under N_2 and cooled (2 hours). The reaction mixture was then added dropwise to the rapidly stirring aqueous solution of sodium dithionite (~0.1 g mL^{-1} in DI water, 25 mL) to reduce all Os complexes to the Os(II) state. The reaction mixture was then chilled on ice and filtered using a fine sintered glass frit (4-5.5 μm) (Pyrex, Corning, NY). Once filtered, the resulting crystals were washed with three aliquots of cold water (5 mL)

and dried on the frit under vacuum (>1 hour), and then in an oven (65 °C, overnight). Oxygen exclusion may result in higher yield.

To form the final Os polymer, $Os(bpy)_2Cl$-PVI, the $Os(bpy)_2Cl_2$ and the PVI components were reacted and then ^{1}H-NMR and cyclic voltammetry (CV) were used to characterize the product. First, $Os(bpy)_2Cl_2$ and PVI were dissolved separately in absolute ethanol (10-15 mL), vortexed, and gently heated. Then, these solutions were combined together in a 100-mL round bottom flask, so the $Os(bpy)_2Cl_2$ was loaded onto the PVI backbone under reflux (1:10 molar ratio Os to imidazole) while stirring in an oil bath (48 hours at 85 °C). The reflux condenser was capped to limit ethanol evaporation during reflux. Then, the reaction mixture was cooled, and ethanol was slowly evaporated under gentle heating and N_2-stream until 6-10 mL were left. The reaction mixture was slowly added dropwise to a stirring solution of diethyl ether (~30 mL) on an ice bath. This Os polymer-ether mixture was then chilled on dry ice, and the precipitate was filtered on a fine sintered glass funnel. This precipitate was then washed with excess volumes (>30 mL) of cold ether to remove unbound $Os(bpy)_2Cl_2$ and dried under vacuum ($<10^{-4}$ Torr, overnight). The product, $Os(bpy)_2Cl$-PVI, was characterized by ^{1}H-NMR (**Supplemental Figure 1**) and CV (**Supplemental Figure 2)** to determine the approximate metal-loading percentage and redox potential, respectively. This product was stored in the dark and was used for all experiments (up to 3 years).

Electrochemical Housing Configuration

Comprised of a screen-printed electrode (SPE) in a flow chamber, the μCA was used for calibrations and sample analysis. SPEs served as the underlying substrate for this platform and were modified for sensitivity and selectivity.[26] The SPE featured three parallel 1.8 mm^2 circular working electrodes, a 19 mm^2 auxiliary electrode, and a 0.08 mm^2 reference electrode, all printed in platinum on a ceramic base. Each working electrode was modified for a specific analyte of interest. Experiments were performed using the modified SPEs in a polymethylmethacrylate flow chamber that was aligned with magnets and compressed with screws. An O-ring sandwiched tightly between the SPE face and the

polymethylmethacrylate created the 26-μL flow chamber, ultimately forming the housing for the SPE, known as the μCA. This apparatus is depicted in detail elsewhere.[22,26]

Electrode Modification

To make these biosensors, reference and working electrodes were generated through electrodeposition and enzyme solution modifications. Initially to make the internal reference electrode, silver was electrodeposited on the electrode followed by immersion in an $FeCl_3$ solution, creating the Ag/AgCl interface with slight modifications from previously developed methods.[26,30] Then, working electrodes had either an Os-polymer-enzyme mixture or a first-generation enzyme solution for comparison deposited on the electrode for detection of glucose or lactate.

To prepare a sensor with an internal reference of Ag/AgCl, a preconditioning step and plating method were performed in a stirring silver nitrate solution (0.3 M $AgNO_3$, 1 M NH_4OH) with an external Ag/AgCl (3 M KCl) reference electrode and a platinum mesh counter electrode. A preconditioning step was first applied (0.3 to 0.95 V, 0.5 V s^{-1}), which was followed by a potential hold (0.95 V, 30 s). Then, the electrode was scanned (0.95 to -0.15 V, 0.5 V s^{-1}) with a subsequent plating potential hold (-0.15 V for 450 s). Following plating, the electrode array was removed from the silver nitrate solution and immediately immersed and agitated in $FeCl_3$ (50 mM, 1 minute) to form a silver chloride layer, generating the internal reference electrode.

Next, an Os-polymer-enzyme mixture was deposited on a working electrode and dried overnight for detection of glucose or lactate. Glucose-specific electrodes were modified using a solution of GOx (0.25 mg mL^{-1} in 50 mM buffer), $Os(bpy)_2Cl$-PVI (50 mg mL^{-1} in 50 mM buffer), and PEGDGE (5% v/v). For instance, 5 μL of a more concentrated GOx solution (0.5 mg mL^{-1} in 50 mM buffer) is added to 4.5 μL of the $Os(bpy)_2Cl$-PVI solution (111 mg mL^{-1} in 50 mM buffer) and 0.5 μL of neat PEGDGE. Lactate-specific electrodes were prepared similarly with PEGDGE (5% v/v), except with LOx (2.5 mg mL^{-1} in 50 mM buffer) and $Os(bpy)_2Cl$-PVI (22.5 mg mL^{-1} in 50 mM buffer). Similarly, for a LOx Os-polymer sensor, 5 μL of a LOx solution (5 mg mL^{-1} in 50 mM buffer) is added to 4.5 μL of the $Os(bpy)_2Cl$-

PVI solution (50 mg mL^{-1} in 50 mM buffer) and 0.5 µL of neat PEGDGE. These solutions were vortexed (5 seconds) in small tubes and then rested to ensure sufficient crosslinking (1 hour, room temperature). These Os-polymer-enzyme solutions were dropcast by pipetting 0.5-µL aliquots onto the working electrodes to create enzyme films. Films were dried at room temperature and then moved to the refrigerator for overnight crosslinking. After the initial use, sensors were then stored (2 °C) in buffered saline solution (2 mM buffer, 120 mM KCl, pH 7.00) to prevent Ag oxidation.

Simultaneously, first-generation enzyme-BSA crosslinked films were prepared similarly for comparative purposes. The sensors were prepared with the same enzyme concentrations used for Os-polymer sensors. However, BSA (31 mg mL^{-1}) in buffer (50 mM) replaced the Os-polymer, and glutaraldehyde (0.25% w/v) replaced the PEGDGE crosslinker in the electrode modification solutions. These solutions were also vortexed (5 seconds) but were immediately deposited, unlike the Os-based sensors. Similar to the procedure for the Os-polymer-enzyme solutions, the enzyme-BSA-glutaraldehyde solutions were dropcast as 0.5-µL aliquots onto the working electrodes to create enzyme films. These sensors were dried at room temperature and stored in the same manner as the previously mentioned Os-polymer sensors.

Sensor Calibrations

Calibrations were completed from glucose, lactate, and APAP standards using a system comprised of automated pumps and valves, the µCA, and a potentiostat. Standards for all three of the chemicals were prepared in buffered saline solution. Each calibrant solution contained increasing quantities of glucose and lactate such that simultaneous calibrations could be performed for the analytes. Comprised of 18 calibrants, the analyte ranges used in this study were 0-23 mM for glucose (**Supplemental Figure 1**) and 0-2.5 mM for lactate, which allowed for the linear range of each analyte to be determined. Separately, APAP was calibrated in the system with five calibrants increasing from 0 to 10 mM APAP for use in later selectivity studies. To establish a baseline for all of the calibrations, the same background buffered saline solution was flowed between every calibrant. A pump and valve system (flow rate of 100 µL min^{-1}) was

used for automation, increased sample/calibrant throughput, and ease of use.[22] The μCA described above was operated in conjunction with the potentiostats to measure the calibrant signals. CHI 1440 and 1030 multichannel potentiostats were used to record the amperometric signals (glucose, lactate, and APAP, sampling frequency of 1 sec^{-1}). The potential for analyte quantification is held at 0.2 V (vs. internal Ag/AgCl) for the Os-based sensors since it is a slightly more oxidative potential relative to the redox potential of the coordination complex – $Os(bpy)_2Cl$-PVI ($Os^{3+/2+}$) or at 0.6 V (vs. internal Ag/AgCl) for the first-generation sensors.

Using linear and non-linear regression of the current versus concentration, limit of quantitation, the maximum limit of linearity, sensitivity of the electrode, maximum rate of reaction, and concentration at 50% saturation of the enzyme were determined. By adding the signal of the blank (buffered saline solution) to ten times the error of the blank and dividing by the sensitivity, the limit of quantitation was determined. To set the upper limit of linearity, the slope between calibration points was used to determine the approximate limit point. Subsequently, the next calibration point was added. If the slope changed by 5% or more from the previous slope without that point then the limit remained the same and the previous datapoint is the maximum limit of linearity.[22] Using the linear range of the data set (limit of quantitation to maximum limit of linearity), a regression of this data set determined the sensitivity of the electrode based on the slope of the line. A non-linear regression was performed on both of the Os-based sensors (glucose and lactate) to determine the maximum rate of reaction for the enzyme, V_{max}, and the concentration at 50% saturation of the enzyme, K_m.

Operational Longevity

Calibrations (7 calibrants within linear range) were completed daily for Os-polymer GOx and LOx sensors to ensure operational longevity for continuously operational systems. Standards for both of the analytes of interest contained increasing quantities of glucose and lactate such that simultaneous calibrations could be performed in buffered saline solution. This same buffered saline solution was also used as the baseline for all of the calibrations and flowed between every calibrant. Similar parameters

were used for the sensor calibrations previously stated above. In short, the same system comprised of automated pumps (flow rate of 100 μL min^{-1}) and valves, the μCA (potential held at 0.2 V vs internal Ag/AgCl), and a potentiostats (CHI 1440/1030) were used in these experiments. However, after each calibration, the sensor was removed from the μCA and stored (2 °C) in buffered saline solution overnight. Then on the next day, another calibration was completed until calibrations for seven days was completed.

Selectivity Assay

A selectivity assay was performed to compare the signal contribution from interference (APAP) and analyte (glucose or lactate) in first-generation and Os-polymer sensors based on selectivity coefficients. The contribution of interference in an amperometric sensor can be represented by a selectivity coefficient, $\boldsymbol{K_{a,i}^{amp}}$, where *a* is the analyte for a specific sensor and *i* is the interferent.[31] The amperometric selectivity coefficient is the quotient of the signal (current) produced from an interferent relative to the interferent concentration, and the current from the analyte relative to the analyte concentration. This relationship is summarized below in Equation 1.

$$\boldsymbol{K_{a,i}^{amp}} = \frac{\frac{i_i}{c_i}}{\frac{i_a}{c_a}} \qquad (1)$$

The signal produced at a certain concentration of the interferent, C_i, is defined as i_i. Similarly, i_a is the current detected for the specific analyte at a defined concentration, C_a. This calculation is used in a comparative study of the Os-polymer sensors and first generation sensors with respect to the analytes and model interferent. By performing a calibration with the Os-based sensors using increasing concentrations of the interferent or analyte independently, the signal contributions of interferent and analyte were separately determined. Then, $\boldsymbol{K_{a,i}^{amp}}$ values for the Os-polymer and first-generation sensors were calculated. The amperometric selectivity coefficients are presented as log($\boldsymbol{K_{a,i}^{amp}}$) values for ease of comparison. Sensors in which the interferent signal dominates over analyte have selectivity values that are positive (APAP-selective), whereas favorable (analyte-selective) coefficients are negative. These values are later used to demonstrate the selectivities of the sensors.

Cell Culture

AML12 cells (ATCC, Manassas, VA) were grown from cryopreserve, incubated, and plated onto a 12-well plate for treatment. The cells were first thawed from a liquid nitrogen cryopreserve and added to warmed media (DMEM/F12 with 10% FBS, 1% p/s, and a primary hepatocyte maintenance supplement kit). Then, the cell suspension was spun down (125 x g, 7 minutes). After discarding the supernatant, 1 mL of media was added to the cell pellet, and the cells were counted. Cells were subsequently added to ~10 mL of media in a T75 flask so that the flask contained ~250,000 cells (50,000 cells mL^{-1}), and it was then incubated (37°C, 5% CO_2). After the cells reached 90% confluency, they were trypsinized (0.25% w/v trypsin-EDTA), spun down (125 x g, 7 minutes), resuspended in media, and plated onto a 12-well plate (50,000 cells mL^{-1}). The cells on the well plate were grown to 90% confluency before treatment.

APAP and Insulin Treatment

To determine the effects of APAP and/or insulin on cellular metabolism, cells were subjected to one of five treatment protocols and then analyzed using the Os-based sensor. One day before the APAP treatment, the AML12 cell media was switched to a minimal media (DMEM/F12, 50% v/v, 5 mM glucose, without both serum and the primary hepatocyte maintenance supplement kit). For treatment, cell media was changed to one of four conditions: minimal media with protocol 1) no additives (media change); protocol 2) APAP only (1.4 mM); protocol 3) insulin only (10 μg mL^{-1}); or protocol 4) APAP and insulin. The treatment media was removed after 2 hours in experiments without insulin and after 24 hours in those containing insulin for analysis by a GOx Os-based sensor. Basal and treatment unconditioned media inputs were also analyzed by both types of sensors for comparison.

Results.

Synthesis and Characterization of the Os- flow rate of 100 μL min^{-1})

Prior to analysis, the Os-polymer was characterized by ^{1}H-NMR and CV. Based on the ratio of proton integration values in the ^{1}H-NMR spectra, the polymer had a metal-loading percentage of 9% (**Supplemental Figure 2**). The redox potential of the Os-based polymer was identified as +156 mV (vs. Ag/AgCl) by CV (**Supplemental Figure 3**). These methods confirmed the structure of the Os-polymer and that it oxidized at a lower potential than APAP as anticipated.[28]

Selectivity Assay

To compare differences between the Os-based sensors presented here and first-generation sensors, selectivities between the analyte and interferent were investigated. Direct comparison of these sensor types indicated the increased selectivity of Os-polymer sensors to the analyte of interest over a model interferent, APAP. The first-generation sensors showed approximately a 0.3-fold selectivity of glucose and 1.79-fold selectivity of lactate over APAP in the same saline buffered solution (**Supplemental Figure 4, left**). In comparison, the Os-based sensors were approximately 40-fold more selective for glucose and 200-fold more selective for lactate over APAP in a saline buffered solution (**Supplemental Figure 4, right**). Therefore, the Os-based sensors have about 2 orders of magnitude (100x) more selectivity for both analytes over first generation sensors.

Sensor Calibrations

Calibrations were performed for glucose and lactate to compare the sensitivities of both types of sensors. The sensitivities of the first-generation and Os-based GOx sensors were 0.166 ± 0.013 μA mM^{-1} and 0.350 ± 0.006 μA mM^{-1}, respectively (**Figure 2, left**). A first-generation LOx sensor showed a sensitivity of 1.71 ± 0.03 μA mM^{-1}, but the Os-polymer LOx sensor had a higher sensitivity at 2.00 ± 0.05 μA mM^{-1} (**Figure 2, right**). Both the Os-based GOx and LOx sensors offered increased sensitivity compared to the first-generation sensors.

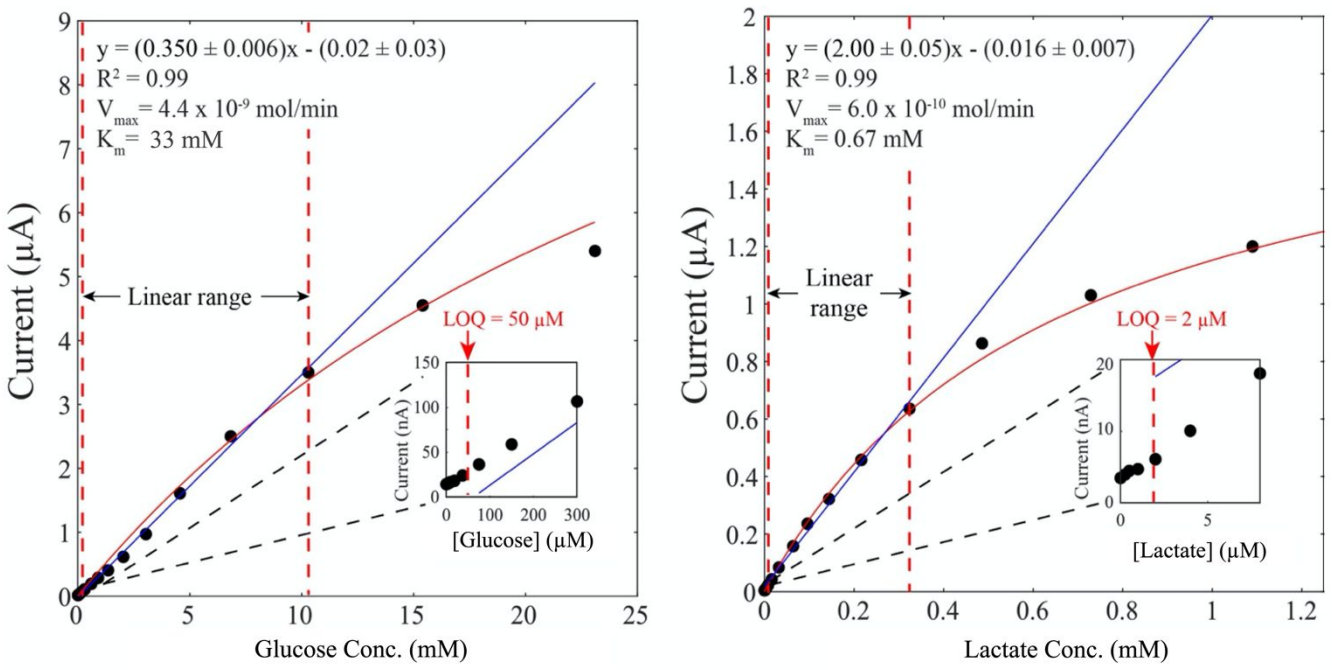

Figure 2. Representative calibration curves of anodic current vs. analyte concentration showing the limits of linearity, limits of quantitation, V_{max}, and K_m for Os-based GOx (left) and LOx (right) sensors. The linear range, indicated by the two dotted red lines, were 50 µM to 10 mM and 2 to 324 µM for glucose and lactate, respectively. The slopes are represented by solid blue lines [y = (0.350 ± 0.006)x – (0.02 ± 0.03), R^2 = 0.99] for the Os-polymer GOx sensor and [y = (2.00 ± 0.05)x – (0.016 ± 0.007), R^2 = 0.99] for the Os-based LOx sensor. Using non-linear regression, shown in solid red, V_{max} and K_m were calculated for both analytes. For the Os-based GOx sensor, V_{max} was 4.4 x 10^{-9} mol min^{-1} and K_m was 33 mM. The Os-polymer LOx had a V_{max} of 6.0 x 10^{-10} mol min^{-1} and K_m of 0.67 mM. Inset: zoom-in of the lower concentrations of each analyte showing the lower limit of linearity (limit of quantitation). Experiments were performed in buffered saline solution (ambient conditions).

To test the linear range of the Os-based sensor, calibrations were performed for both glucose and lactate. Glucose was detected as low as 43 µM and quantified as low as 50 µM. At higher concentrations of glucose, the data began to deviate from linearity at ~10 mM, so the linear range was 50 µM to 10 mM (**Figure 2, left**). Non-linear regression identified the V_{max} and K_m for glucose as 4.4 x 10^{-9} mol min^{-1} and 32.9 mM, respectively. Similarly, the newly developed lactate sensor was tested to determine the linear

range. The limit of detection was 1 μM while the limit of quantitation was 2 μM for lactate. The data began to deviate from linearity at 324 μM. Based on a non-linear regression model of the data, the V_{max} and K_m were 6.0 x 10^{-10} mol min^{-1} and 0.67 mM, respectively. Therefore, the linear range for the lactate sensor spanned from 2 to 324 μM (**Figure 2, right**). Both of the Os-based sensors offered a wide biologically-relevant linear range.

Operational Longevity

The sensitivities of the Os-based sensors were monitored over time to investigate the long-term stability of sensor performance. To do this, a calibration was carried out daily for a week for the Os-based GOx and LOx sensors. The sensitivity of the GOx sensor decreased from 420 ± 7 nA mM^{-1} to 313 ± 7 nA mM^{-1}, a 26% decrease, while the sensitivity decreased from 2460 ± 70 nA mM^{-1} to 1730 ± 70 nA mM^{-1}, a 29% decrease for the LOx sensor over the weeklong experiment (**Figure 3**).

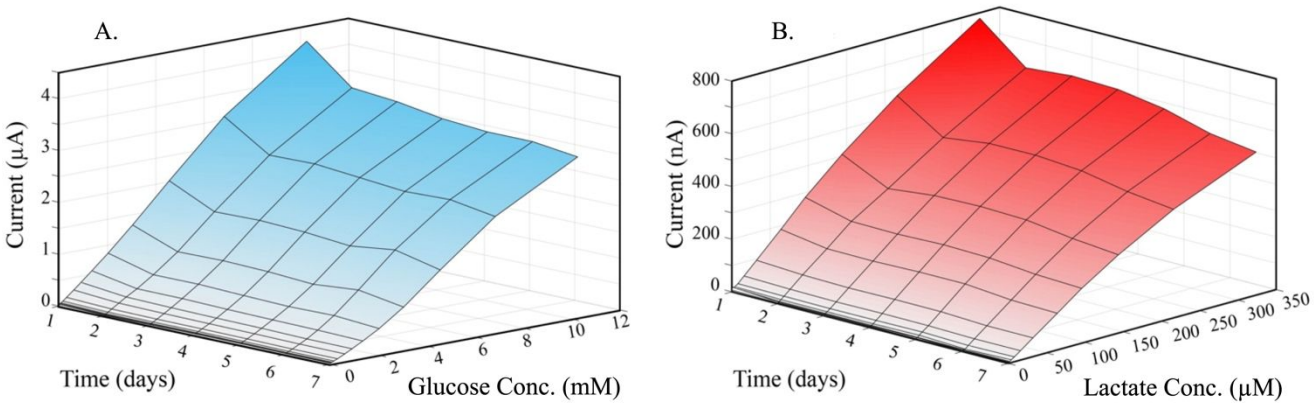

Figure 3. Operational longevity of the Os-based GOx (A) and LOx (B) sensors was tested by calibrating daily for seven days. Anodic (oxidative) current vs. calibration day vs. analyte concentration reported above. The sensitivity of the GOx sensor decreased from 420 ± 7 nA mM^{-1} to 313 ± 7 nA mM^{-1}, and the LOx sensor sensitivity decreased from 2460 ± 70 nA mM^{-1} to 1730 ± 70 nA mM^{-1} in the course of the week. Experiments were performed in buffered saline solution (ambient conditions) at 0.2 V. Data represented as the average, n = 3 replicates.

APAP and Insulin Treatment

To test the biological relevance of the Os-polymer sensors, AML12 glucose metabolism was observed with and without the addition of a background interferent. A glucose concentration above 5 mM (basal media concentration) denotes produced glucose while a glucose concentration below 5 mM signifies consumed glucose. Four control media samples were measured for glucose using the Os-polymer sensor. The basal media was treated with: protocol 1) no additives (4.78 ± 0.09 mM glucose, **Figure 4, solid blue**); protocol 2) added APAP (4.91 ± 0.05 mM glucose); protocol 3) added insulin (4.63 ± 0.14 mM glucose); and protocol 4) added both APAP and insulin (4.79 ± 0.10 mM glucose). These values are not significantly different ($p = 0.28$), so the basal media without additives is shown below as a representative for the control media. When compared to the control media, cells cultured in only basal media, protocol 1, and basal media with APAP, protocol 2, showed increased concentrations of glucose (7.15 ± 0.06 mM glucose and 6.78 ± 0.09 mM glucose, respectively) when compared to the control media (**Figure 4, striped**). In contrast, the glucose concentration decreased in cells challenged with protocol 3, media with insulin, (4.43 ± 0.11 mM glucose) and protocol 4, insulin-containing media from APAP-treated cells (3.83 ± 0.09 mM glucose, **Figure 4, checkered**) when compared to the control media.

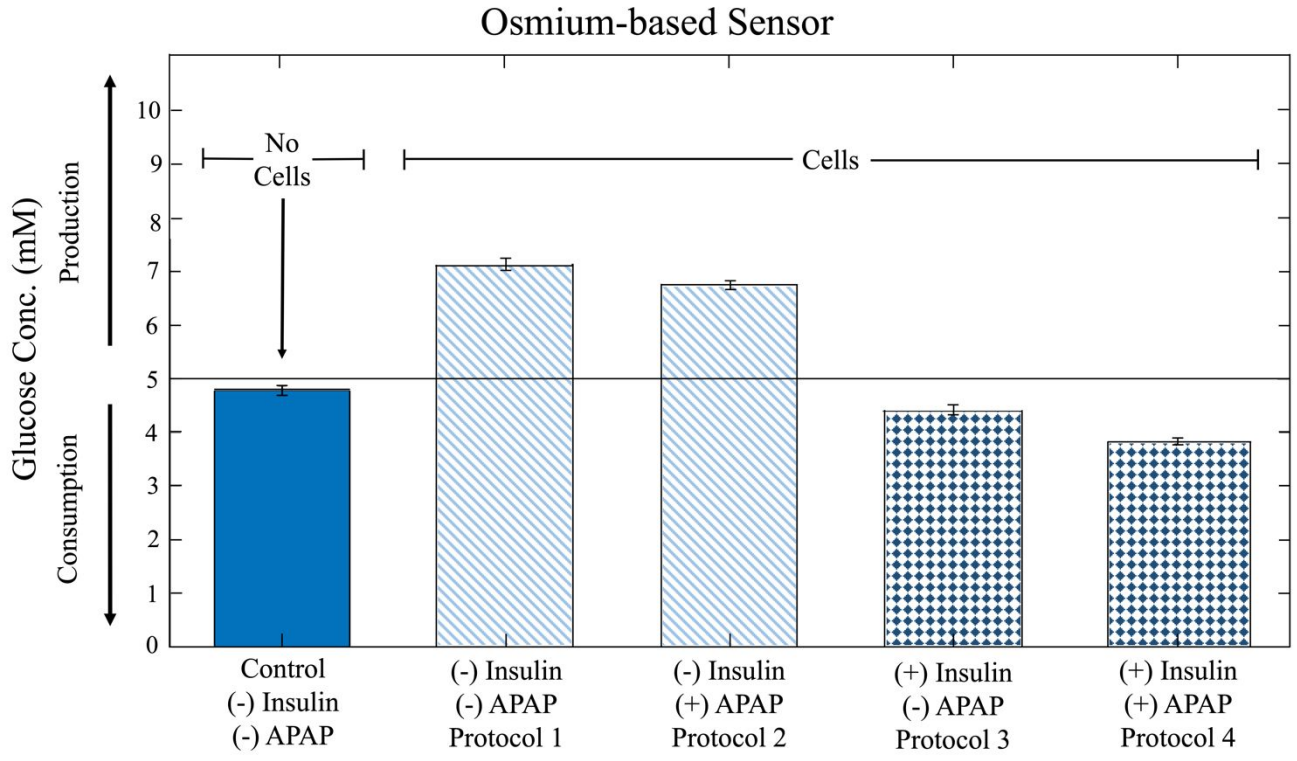

Figure 4. Bar graph displaying the glucose concentration analyzed using an Os-based sensor vs. sample type including control and cellular samples. AML 12 cells were grown to 90% confluency in four different growth protocols and their glucose metabolism was monitored using the Os-based sensor and compared to a control without cells. Reduced glucose media is shown as the control with 4.78 ± 0.09 mM glucose. Cellular media without insulin was analyzed after two hours of exposure and is represented with stripes. Protocol 1 was the cellular media (reduced glucose DMEM/F12) without APAP and had 7.15 ± 0.06 mM glucose. Denoted as protocol 2, cells treated with APAP (1.4 mM) had 6.78 ± 0.09 mM glucose. The samples, illustrated with diamonds, were cultured in insulin-containing media and analyzed after 24 hours of exposure. The cells cultured in media with insulin (10 μg mL^{-1}) but without APAP were protocol 3 and had 4.43 ± 0.11 mM glucose, while the media from insulin- (10 μg mL^{-1}) and APAP- (1.4 mM) treated cells was protocol 4 and had 3.84 ± 0.09 mM glucose. Experiments were performed in reduced glucose DMEM/F12 media (ambient conditions). Data represented as an average and standard error with n = 3 biological replicates.

To determine the effect of insulin on glucose metabolism, AML12 cells were cultured with and without insulin and analyzed by the Os-polymer sensor. Glucose concentration changes due to the addition or removal of insulin were compared between cells treated the same (basal media or APAP-added). In comparing the cells that were left untreated and were either cultured with insulin (4.43 ± 0.11 mM glucose) or without it (7.15 ± 0.06 mM glucose), the glucose metabolism showed a significant difference ($p < 0.01$). Similarly, the APAP-treated cells were significantly different in glucose metabolism between those with (3.83 ± 0.09 mM glucose) and without insulin (6.78 ± 0.09 mM glucose) in the media ($p < 0.01$). Cells that were cultured without insulin had a larger glucose concentration than those with it.

While further examining glucose metabolism, the effect of APAP was analyzed using the Os-polymer sensor by treating cells with either basal media alone (untreated) or basal media with APAP. Samples from the media without insulin had a significantly decreased glucose concentration ($p < 0.01$)

for those cells treated with APAP (6.78 ± 0.09 mM glucose) compared to the untreated cells (7.15 ± 0.06 mM glucose). The untreated cells (4.43 ± 0.11 mM glucose) had significantly increased glucose compared to the APAP-treated cells (3.83 ± 0.09 mM glucose) in media containing insulin as well ($p < 0.02$). Based on these results, the APAP-treated cells have less glucose in the media compared to the untreated cells.

To demonstrate the decreased sensitivity of the Os-based sensor to the model interferent basal media with and without APAP was analyzed using both types of sensors. When analyzed by a first-generation sensor, the basal media with insulin (3.0 ± 0.6 mM glucose) had a lower glucose concentration than the same basal media and insulin with added APAP (24 ± 2 mM glucose) (**Supplemental Figure 5**). There was a significant difference in the basal media with and without APAP ($p < 0.01$). However, the same comparison between basal media with insulin (4.63 ± 0.14 mM glucose) and basal media with insulin and APAP (4.79 ± 0.10 mM glucose), but analyzed by an Os-based GOx sensor was not significantly different ($p = 0.44$). Since the Os-based sensors did not show significantly different results while the first-generation sensors did, it was confirmed the Os-based sensors had decreased sensitivity to APAP.

Discussion.

Electrochemical microphysiometry is an effective method in studying cellular bioenergetics and toxicity.[32] However, electroactive signal interference may prevent accurate detection of the analytes of interest. In this work, Os-polymer sensors were used to mitigate interference by reducing the potential bias of the electrode. These sensors showed high analyte-selectivity, had a biologically-relevant linear range with increased sensitivity for the analyte compared to first-generation sensors, and established operational stability for use with model organ-on-chip systems. Together with the μCA, this system provided an easy-to-use and versatile format for sensing metabolites to improve diagnosing and monitoring health and disease.[1–3]

First, selectivities between the analyte and interferent were investigated for the developed Os-based sensors for comparison with the first-generation sensors. These Os-based sensors were approximately two orders of magnitude more selective than first-generation sensors for both analytes, demonstrating the reduced interference from APAP due to the presence of the Os-polymer that allowed for a reduced potential bias. Because the Os-based sensors were less affected by the interferent, the results from these sensors provided more accurate details about the system. This interferent insensitivity makes the high-resolution Os-polymer sensors ideal for monitoring changes in multiple biological analytes over a high background of an electroactive interferent, APAP.

Both of the new Os-based biosensors for glucose and lactate showed higher selectivity for their respective analytes compared to the redox-active interferent, APAP, since the Os-polymer allowed for a lower potential to be applied at the electrode surface. Because the Os-polymer biosensors were operated at 0.2 V (vs. Ag/AgCl), minimal APAP signal was generated. This reduced signal is expected, because 0.2 V (vs. Ag/AgCl) is well below the potential threshold for bulk APAP oxidation. Conversely, the 0.6 V (vs. Ag/AgCl) electrode bias required to transduce a signal from the O_2-H_2O_2 couple in first-generation sensors was high enough to oxidize interferents in the solution. Additionally, the observation of an anodic (negative) current in these sensors confirmed the predicted electron flow mechanism (**Figure 1**), in which

electron donation occurs first from the oxidase enzyme to the reduced osmium (Os^{3+}) complex and finally to the SPE.

These polymers not only decrease interference, they are also predicted to improve sensitivity of the sensor over first-generation sensors. Os-based GOx sensors have shown to have better sensitivity compared to first-generation GOx sensors (**Supplemental Figure 6**). Because there are increase amine sites because of the imidazole there is increased crosslinking and increased electron transfer. $Os(bpy)_2Cl$-PVI had higher crosslinking efficiency with increased amine sites from the imidazole in the polymer while maintaining higher electron transfer from the osmium complex. Covalent linking of the enzyme to the hydrogel provided an enhanced pathway for electron transfer, thus increasing the sensitivity of the Os-based sensors compared to first-generation sensors.[33]

Further evidence for the advantage of the Os-based sensors was the improved sensitivity while simultaneously spanning a large linear range necessary for monitoring a variety of biological processes. The first-generation sensors had a lower sensitivity for both glucose and lactate compared to the Os-polymer sensors. As predicted, the Os-polymer mediates an enhanced electron pathway, producing a higher sensitivity. More specifically, there was a 111% increase in sensitivity for the Os-polymer GOx sensors and a 17% increase in the sensitivity for Os-based LOx sensors compared to their respective first-generation sensors. This increased sensitivity allowed for a low level of detection and quantitation while still including higher concentrations which are both necessary for model organ systems and other biological applications. While there was slightly less sensitivity for Os-based glucose sensors compared to previous Os-polymer sensor, there was an improved sensitivity for the Os-based LOx sensors.[34,35] Based on previous data, the V_{max} value for the glucose Os-based sensor was similar to that of a first-generation, but the lactate Os-polymer sensor was a magnitude less than a first-generation sensor.[36] The lactate sensor does not need to measure as high as the glucose so a lower V_{max} value is acceptable.[26] Furthermore, the Os-polymer GOx sensor had a higher limit of quantitation but also had a much higher limit of linearity compared to a previously developed glucose Os-based sensor.[37] This is helpful when

using media that has higher glucose concentrations in it such as in this work with the AML12 cells. In addition, both types of these Os-polymer sensors had a higher limit of detection but a lower limit of linearity when compared to first-generation sensors.[26] These sensors offered improved sensitivity and a wide linear range for glucose (50 μM to 10 mM) and lactate (2 to 324 μM) that is suitable for monitoring cellular function and biological processes.[1–3,38–42]

Finally, considering the utility of this sensor platform in tandem with a continuously operational system, the longevity of sensor performance was investigated. In both sensors, after an expected initial sensitivity decrease was observed from enzymatic activity loss, the sensitivity decreased slightly and stayed stable over the weeklong study (**Supplemental Figure 7**). These sensitivity decreases were expected in first-generation sensors as well, so the operational stability was not compromised by the addition of the Os-polymer.[26] First-generation sensors have been tested previously for longevity, showing loss of sensitivity attributed to enzyme degradation.[26] Although the first-generation sensors showed they could be used up to three weeks for glucose and two weeks for lactate, the current Os-based sensors were only tested for seven days and may have longer operational longevity than tested.[26] Furthermore, the electrodes still yielded a significant analyte response, upon which a new calibration curve was prepared. Another Os-based glucose sensor showed similar stability of a week as the Os-based sensor presented here.[37] The slight decrease in sensitivity throughout the week emphasized the need for regular recalibration in continuously operational sensors. These sensors may be promising for their use in monitoring multiple biological analytes over extended periods of time.

The culturing media dysregulated glucose metabolism of AML12 cells with the addition or removal of insulin. The cells cultured in media with insulin had decreased glucose concentrations when compared to control media. Presumably, the cells were consuming glucose and exhibiting the regular insulin-stimulated glucose metabolism shown in AML12 cells.[25] Both of the samples without insulin showed increased concentrations of glucose compared to the control media. Therefore, glucose was produced, which is consistent with previous results from AML12 cells without insulin.[24,25] These results

validate the Os-based sensor as an accurate detection method. Glucose metabolism of AML12 cells reversed with the addition of insulin to the culturing media.

Glucose metabolism of treated and untreated AML12 cells was investigated with a background interferent to test the Os-polymer sensors' biological relevance and application to model organ systems. Because there is a risk of liver damage with a blood level of APAP at 200 μg/mL (1.3 mM for the average person) after four hours of ingestion, a concentration of 1.4 mM APAP was chosen to induce liver changes in glucose metabolism.[43] Both sets of APAP-treated cell media had a lower glucose concentration than the accompanying untreated cells, indicating the APAP-treated cells had dysregulated glucose metabolism. The cells were likely consuming more glucose to compensate for the stress of APAP exposure and the onset of toxicity, thus changing the glucose metabolism of the cell. Therefore, we accurately measured glucose metabolism in the presence of APAP and showed the dysregulation due to the toxicant with the Os-based sensor.

Finally, a comparison of the two different sensors was investigated, highlighting the strength of the Os-polymer sensors to mitigate interference. There was a large difference between the basal media with and without APAP when analyzed by the first-generation sensor, but no difference is seen in the same media samples analyzed by the Os-based sensors. This juxtaposition emphasized the increased resolution of the developed sensors while maintaining the integrity of the sensor for a more accurate detection method than first-generation sensors.

Conclusions.

A new multianalyte biosensor platform was constructed to directly quantify changes in glucose and lactate over high backgrounds of an electroactive interferent, APAP. Os-based redox hydrogels were utilized to mediate electron transport from the enzyme to the electrode, reducing the need for high electrode potentials, and therefore mitigating the effects of APAP on the electrochemical signal. Flow-based experiments using the μCA were performed simultaneously for glucose and lactate Os-based sensors. The automation that the μCA offers and the addition of these sensors to the ever-expanding toolbox of measurable analytes provides an efficient and versatile format. Selectivity assays indicated greatly diminished signal contributions from interferent with improved sensitivity in the Os-based sensors when compared to first-generation biosensors. The Os-polymer sensors offered a wide linear range that can be used for measuring changes in the metabolic profile of biological systems. Finally, long-term performance evaluations revealed that these sensors retain substantial analytical sensitivity after several days of use and storage, indicating that this platform can successfully be integrated in-line with a biological system for analysis. The results from cellular experiments indicated 1) the removal of insulin from basal media reversed glucose metabolism in AML12 cells; 2) APAP reduced production of glucose in the cells; and 3) the Os-based sensor had diminished signal interference compared to the first-generation sensor. This high-resolution platform can easily be translated to other applications such as glucose meters for diabetics,[7] lactate sensors for the food industry,[44] and biomimicry for pharmaceuticals (organs-on-chips).[45–49]

Supplementary Information.

1. ^{1}H-NMR of Poly(N-vinylimidazole-allylamine) and Os(bpy)$_2$Cl-PVI
2. Cyclic Voltammogram of Os(bpy)$_2$Cl-PVI
3. Selectivity Assay Graph Comparing Synthesized Os-Polymer Sensors and First-Generation Sensors
4. Comparison of Control Media with First-Generation Sensors

Author contributions.

S.L.M. contributed to experimental design, executed experiments, interpreted results, and wrote the manuscript. D.R.M. and E.A.G. executed experiments and wrote the manuscript. D.E.C. contributed to experimental design and wrote the manuscript.

Acknowledgements.

The authors thank Dr. Nathan Schley and Margaret Calhoun from Vanderbilt University for assistance with the polymer. The authors graciously acknowledge financial support from the Defense Threat Reduction Agency (DTRA) under award CBMXCEL-XL1-2-0001, and the Environmental Protection Agency (EPA-83573601). E.A.G. was supported in part by funding provided by the Vanderbilt University Mitchum E. Warren and Frederic LeRoy Conover Graduate Research Fellowships. This work was also supported in part by the National Institute of Health training grant (ES007028) for funding S. L. M., EPA (83573601), and IARPA (2017-17081500003) and using the resources of the Vanderbilt Microfabrication Core operated by the Vanderbilt Institute for Integrative Biosystems Research and Education.

Disclaimer.

This article reflects the views of the authors and should not be construed to represent the views or policies of the DTRA, NIH, EPA, or IARPA.

References.

1 A. Heller and B. Feldman, *Chem. Rev.*, 2008, **108**, 2482–2505.

2 S. C. Perry, S. M. Gateman, J. Sifakis, L. Pollegioni and J. Mauzeroll, *J. Electrochem. Soc.*, 2018, **165**, G3074–G3079.

3 O. Smutok, M. Karkovska, H. Smutok and M. Gonchar, *ScientificWorldJournal.*, 2013, **2013**, 461284.

4 D. W. Kimmel, G. LeBlanc, M. E. Meschievitz and D. E. Cliffel, *Anal. Chem.*, 2012, **84**, 685–707.

5 E. S. McLamore, J. Shi, D. Jaroch, J. C. Claussen, A. Uchida, Y. Jiang, W. Zhang, S. S. Donkin, M. K. Banks, K. K. Buhman, D. Teegarden, J. L. Rickus and D. M. Porterfield, *Biosens. Bioelectron.*, 2011, **26**, 2237–2245.

6 J. Wang, *Chem. Rev.*, 2008, 108, 814–825.

7 A. Basu, S. Veettil, R. Dyer, T. Peyser and R. Basu, *Diabetes Technol. Ther.*, 2016, **18 Suppl 2**, S243-7.

8 S. K. Smith, C. A. Lee, M. E. Dausch, B. M. Horman, H. B. Patisaul, G. S. McCarty and L. A. Sombers, *ACS Chem. Neurosci.*, 2017, **8**, 272–280.

9 J. Wang, *Chem. Rev.*, 2008, **108**, 814–825.

10 L. Xiao, J. Chen and C. Cha, *J. Electroanal. Chem.*, 2000, **495**, 27–35.

11 H. Deng, A. K. L. Teo and Z. Gao, *Sensors Actuators B Chem.*, 2014, **191**, 522–528.

12 S. Bharathi and M. Nogami, *Analyst*, 2001, **126**, 1919–1922.

13 T. Dodevska, E. Horozova and N. Dimcheva, *Anal. Bioanal. Chem.*, 2006, **386**, 1413–1418.

14 H. Sakslund, J. Wang, F. Lu and O. Hammerich, *J. Electroanal. Chem.*, 1995, **397**, 149–155.

15 G. Yu, W. Wu, X. Pan, Q. Zhao, X. Wei and Q. Lu, *Sensors*, 2015, **15**, 2709–2722.

16 Y. Degani and A. Heller, *J. Am. Chem. Soc.*, 1989, **111**, 2357–2358.

17 T. J. Ohara, R. Rajagopalan and A. Heller, *Anal. Chem.*, 1993, **65**, 3512–3517.

18 S. Kurbanoglu, M. N. Zafar, F. Tasca, I. Aslam, O. Spadiut, D. Leech, D. Haltrich and L. Gorton,

Electroanalysis, 2018, **30**, 1496–1504.

19 P. Bollella, L. Medici, M. Tessema, A. A. Poloznikov, D. M. Hushpulian, V. I. Tishkov, R. Andreu, D. Leech, N. Megersa, M. Marcaccio, L. Gorton and R. Antiochia, *Solid State Ionics*, 2018, **314**, 178–186.

20 L. Mao and K. Yamamoto, *Electroanalysis*, 2000, **12**, 577–582.

21 T. Kato, J. K. Liu, K. Yamamoto, P. G. Osborne and O. Niwa, *J. Chromatogr. B Biomed. Sci. Appl.*, 1996, **682**, 162–166.

22 D. R. Miller, E. S. McClain and D. E. Cliffel, *J. Electrochem. Soc.*, 2018, **165**, G3120–G3124.

23 R. S. Sherwin, *Diabetes Care*, 1980, **3**, 261–265.

24 S. Sefried, H.-U. Häring, C. Weigert and S. S. Eckstein, *Open Biol.*, 2018, **8**, 180147.

25 S. R. Nagarajan, M. Paul-Heng, J. R. Krycer, D. J. Fazakerley, A. F. Sharland, X. Andrew and J. Hoy, *Am J Physiol Endocrinol Metab*, 2019, **316**, 578–589.

26 J. R. McKenzie, A. Cognata, A. N. Davis, J. P. Wikswo and D. E. Cliffel, *Anal. Chem.*, 2015, 150630093637003.

27 A. Badura, D. Guschin, B. Esper, T. Kothe, S. Neugebauer and W. Schuhmann, *Electroanalysis*, 2008, **20**, 1043–1047.

28 M. N. Zafar, X. Wang, C. Sygmund, R. Ludwig and L. Gorton, *Anal. Chem.*, 2012, **84**, 334.

29 E. M. Kober, J. V Caspar, B. P. Sullivan and T. J. Meyer, *Inorg. Chem.*, 1988, **27**, 4587–4598.

30 B. J. Polk, A. Stelzenmuller, G. Mijares, W. MacCrehan and M. Gaitan, *Sensors Actuators, B Chem.*, 2006, **114**, 239–247.

31 J. Wang, *Talanta*, 1994, **41**, 857–863.

32 A. N. Davis, A. R. Travis, D. R. Miller and D. E. Cliffel, *Annu. Rev. Anal. Chem*, 2017, **10**, 93–111.

33 K. H. Cha and M. E. Meyerhoff, 2018, **28**, 32.

34 T.-M. Park, E. I. Iwuoha, M. R. Smyth, R. Freaney and A. J. McShane, *Talanta*, 1997, **44**, 973–

978.

35 T. J. Ohara, R. Rajagopalan and A. Heller, *Anal. Chem.*, 1994, **66**, 2451–2457.

36 S. E. Eklund, D. Taylor, E. Kozlov, A. Prokop and D. E. Cliffel, *Anal. Chem.*, 2004, **76**, 519–527.

37 R. Antiochia and L. Gorton, *Biosens. Bioelectron.*, 2007, **22**, 2611–2617.

38 M. Winter and R. J. Brodd, *Chem. Rev.*, 2004, **104**, 4245–4269.

39 J. Hollaender, *Food Addit. Contam.*, 1997, **14**, 617–626.

40 M. Pourbaix, *Corros. Sci.*, 1974, **14**, 25–82.

41 X. Hu and S. Dong, *J. Mater. Chem.*, 2008, **18**, 1279.

42 P. H. Gamache, D. F. Meyer, M. C. Granger and I. N. Acworth, *J. Am. Soc. Mass Spectrom.*, 2004, **15**, 1717–1726.

43 Acetaminophen Drug Level - Health Encyclopedia - University of Rochester Medical Center, https://www.urmc.rochester.edu/encyclopedia/content.aspx?contenttypeid=167&contentid=acetaminophen_drug_level, (accessed 30 April 2020).

44 I. Bravo, M. Revenga-Parra, F. Pariente and E. Lorenzo, *Sensors (Basel).*, , DOI:10.3390/s17010144.

45 A. S. Kalgutkar and J. R. Soglia, *Expert Opin. Drug Metab. Toxicol.*, 2005, **1**, 91–142.

46 M. Eisenstein, *Nature*, 2015, **519**, S16–S18.

47 V. Marx, *Nature*, 2015, **522**, 373–377.

48 B. R. Ware and S. R. Khetani, , DOI:10.1016/j.tibtech.2016.08.001.

49 M. S. Hutson, P. G. Alexander, V. Allwardt, D. M. Aronoff, K. L. Bruner-Tran, D. E. Cliffel, J. M. Davidson, A. Gough, D. A. Markov, L. J. McCawley, J. R. McKenzie, J. A. McLean, K. G. Osteen, V. Pensabene, P. C. Samson, N. K. Senutovitch, S. D. Sherrod, M. S. Shotwell, D. L. Taylor, L. M. Tetz, R. S. Tuan, L. A. Vernetti and J. P. Wikswo, *Appl. Vitr. Toxicol.*, 2016, **2**, 97–102.

ToC Image:

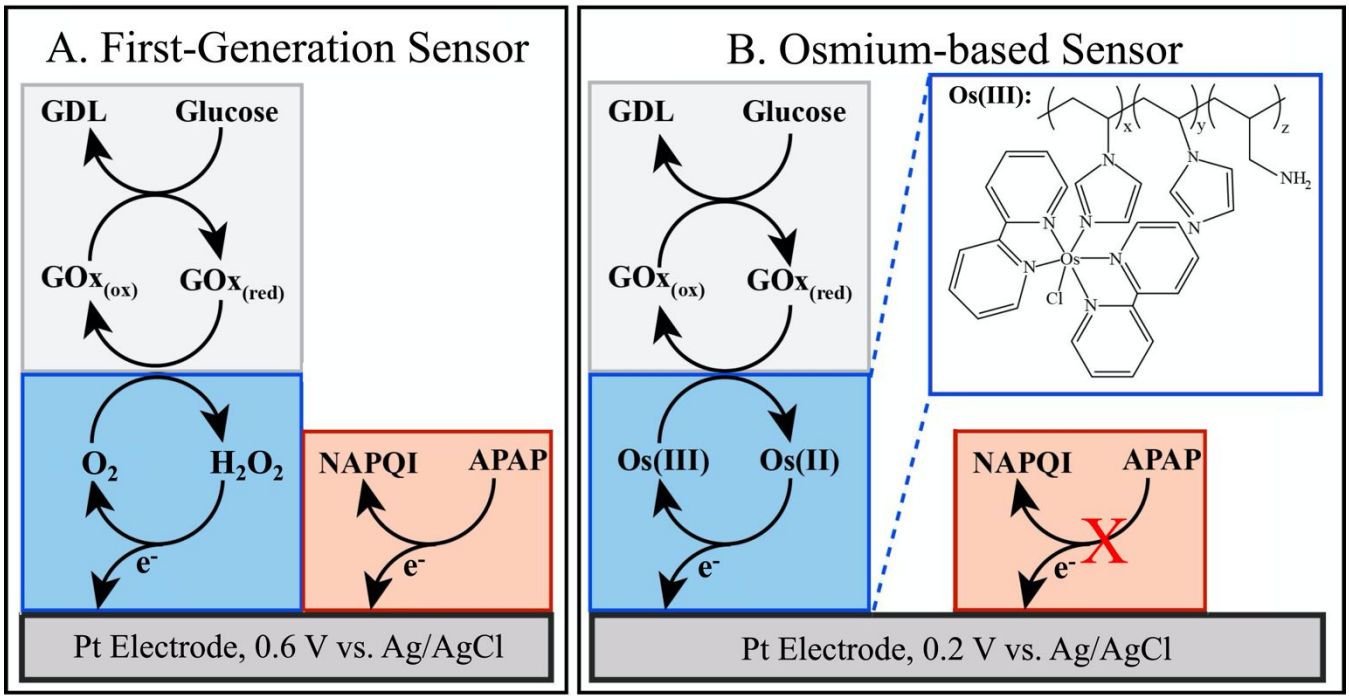
A. First-Generation Sensor
GDL
Glucose
GOx(ox)
GOx(red)
O2
H2O2
e-
NAPQI
APAP
e-
Pt Electrode, 0.6 V vs. Ag/AgCl
B. Osmium-based Sensor
GDL
Glucose
GOx(ox)
GOx(red)
Os(III):
NH2
Os(III)
Os(II)
e-
NAPQI
APAP
X
e-
Pt Electrode, 0.2 V vs. Ag/AgCl